



**HAL**  
open science

# Topology-preserving conditions for 2D digital images under rigid transformations

Phuc Ngo, Yukiko Kenmochi, Nicolas Passat, Hugues Talbot

► **To cite this version:**

Phuc Ngo, Yukiko Kenmochi, Nicolas Passat, Hugues Talbot. Topology-preserving conditions for 2D digital images under rigid transformations. *Journal of Mathematical Imaging and Vision*, 2014, 49 (2), pp.418-433. 10.1007/s10851-013-0474-z . hal-00838183v2

**HAL Id: hal-00838183**

**<https://hal.science/hal-00838183v2>**

Submitted on 23 Sep 2014

**HAL** is a multi-disciplinary open access archive for the deposit and dissemination of scientific research documents, whether they are published or not. The documents may come from teaching and research institutions in France or abroad, or from public or private research centers.

L'archive ouverte pluridisciplinaire **HAL**, est destinée au dépôt et à la diffusion de documents scientifiques de niveau recherche, publiés ou non, émanant des établissements d'enseignement et de recherche français ou étrangers, des laboratoires publics ou privés.

# Topology-preserving conditions for 2D digital images under rigid transformations

Phuc Ngo · Yukiko Kenmochi · Nicolas Passat · Hugues Talbot

Received: date / Accepted: date

**Abstract** In the continuous domain  $\mathbb{R}^n$ , rigid transformations are topology-preserving operations. Due to digitization, this is not the case when considering digital images, *i.e.*, images defined on  $\mathbb{Z}^n$ . In this article, we begin to investigate this problem by studying conditions for digital images to preserve their topological properties under all rigid transformations on  $\mathbb{Z}^2$ . Based on (i) the recently introduced notion of DRT graph, and (ii) the notion of simple point, we propose an algorithm for evaluating digital images topological invariance.

**Keywords** Rigid transformation · 2D digital image · discrete topology · simple point · DRT graph

## 1 Introduction

Rigid transformations (*i.e.*, rotations composed with translations) are involved in numerous 2D and 3D image processing and analysis tasks, for instance in registration [1] and tracking [2]. In such applications, the images are necessarily digital, and can then be considered as functions  $I : \mathbb{S} \rightarrow \mathbb{V}$  from a finite subset  $\mathbb{S} \subset \mathbb{Z}^n$  to a value space  $\mathbb{V}$ .

Rigid transformations are topology-preserving in  $\mathbb{R}^n$ . By “topology-preserving”, we mean that they do not alter intrinsic structural properties, generally modeled by topological invariants (*e.g.*, Euler characteristic, homotopy-type, fundamental groups, etc.). Unfortunately, this property, which is highly desirable in image analysis and processing, is generally lost in  $\mathbb{Z}^n$ . Typically, digital rigid transformations (*i.e.*,

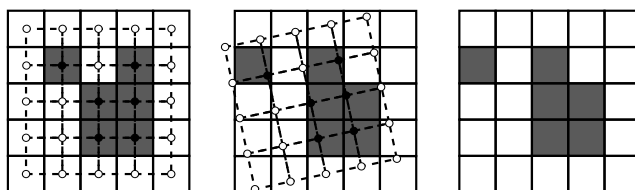


**Fig. 1** Left: binary digital image and the grid modeling its discrete structure. Middle: a rigid transformation applied on this grid. Right: the resulting transformed image, which is not topologically identical to the initial image (for instance, if considered 8-connected, the black component was split).

rigid transformations followed by a digitization process) alter, in most cases, the topological properties of digital images, such as the homotopy-type, as exemplified in Fig. 1. This is due to the sampling effects induced by the mandatory digitization process from  $\mathbb{R}^n$  to  $\mathbb{Z}^n$ .

Several works have been devoted to topology-preserving transformations, in particular in the context of image warping [3,4], and atlas-based segmentation [5], where topology preservation is a crucial issue. However topology preservation in the case of rigid transformations in images has not yet been considered. In this article – that is an extended and improved version of the conference paper [6] – we study this specific issue. More precisely, we focus on the 2D case, and on defining some conditions for digital images such that their homotopy-type is preserved under all rigid transformations.

To this end, we consider the notion of DRT graph, that we recently introduced and studied from a theoretical point of view in [7]. It defines a combinatorial model of all the rigid transformations of a 2D digital image. We also consider the classical notion of simple points, which can be used to guarantee the preservation of homotopy-type, and has been extended to several categories (binary, grey-level, labeled) of digital images. By combining these two notions,

Phuc Ngo (corresponding author), Yukiko Kenmochi, Hugues Talbot  
Université Paris-Est, LIGM, UPEMLV-ESIEE-CNRS, France  
Tel.: +33-145926737  
Fax: +33-145926699  
E-mail: ngoh@esiee.fr

Nicolas Passat  
Université de Reims Champagne-Ardenne, CReSTIC, France

we provide a combinatorial analysis of 2D digital image topology under rigid transformations. The basic idea of the proposed method is to generate all the transformed images using the DRT graph, and simultaneously evaluate their homotopy-type preservation using the notion of simple points. This analysis finally leads us to an efficient algorithm for evaluating the homotopy-type preservation of digital images under all rigid transformations.

The article is organized as follows. The state of the art in both digital rigid transformation and topology preservation is exposed in Sec. 2. Basic definitions and notations are provided in Sec. 3. In Sec. 4, we introduce the main issues related to topology alterations induced by the embedding of rigid transformations into digital spaces. Our contribution is exposed in Secs. 5–7. Specifically, in Sec. 5, we introduce the DRT graph [7] as a tool for studying the behaviour of rigid transformations on digital images from a topological point of view. In particular, we propose a first algorithm for assessing the topological invariance of a digital image under all possible rigid transformations, with a superlinear time and space complexity, corresponding to that of the associated DRT graph. In Sec. 6, we refine this first approach, by spatially decomposing the image analysis process, leading to an equivalent algorithm that presents a low complexity with respect to the image size. In Sec. 7, this method is experimentally assessed in terms of complexity and correctness. Sec. 8 finally summarizes the contributions and proposes some future work.

## 2 State of the art

### 2.1 Rigid transformations on digital images

To reach our stated goal of finding conditions for topology preservation of digital images under all rigid transformations, it is necessary to compare the topological properties of the initial image and all of its transformed images. Studying the problem in the continuous domain is however unfeasible due to the uncountable number of transformations in  $\mathbb{R}^2$ , and so a discrete method must be devised, preferably involving only integer operations for exactness.

Over the last two decades, several methods were proposed to study transformations on digital images as fully discrete processes. In particular, different studies in combinatorial analysis for the problem of 2D pattern matching under different classes of geometric transformations have been considered for: rotations [8,9]; scalings [10,11]; combined scalings and rotations [12]; affine transformations [13,14]; projective and linear transformations [15]. To the best of our knowledge, fully discrete approaches devoted to rigid transformations are in quite limited number.

Digital rigid transformations include discrete rotations. For this class, one can cite the quasi-shear rotations [16,17]

which were introduced to preserve bijectivity. The approach consists of decomposing a rotation into three horizontal or vertical quasi-shears in order to obtain a discrete transformation. Based on this strategy, this quasi-shear composition however trades bijectivity for transitivity. As a consequence, the result obtained by a quasi-shear rotation is not always identical to the result obtained by applying a Euclidean rotation followed by a discretization.

In this article, we propose an alternative approach that provides the same discretized result as the Euclidean discretized method, but we do not guarantee bijectivity. For this purpose, a discrete formulation of rotations based on hinge angles has been proposed in [18–21]. Informally, for a discrete finite set, rotations around a fixed center and with “small” angle variations will not result in any change. Conversely, some larger angle rotations will indeed result in pixel modifications. The notion of hinge angles formalizes this property. In particular, hinge angles (represented by integer triplets) hold sufficient information for incrementally generating and performing all rotations.

Following the idea of rotations by hinge angles and inspired by the discretization technique of the problem of 2D pattern matching, we have recently studied in [7] the combinatorial aspects and properties of the class of rigid transformations, by simultaneously considering the parameter space for both translations and rotations. Our approach discretizes the induced parameter space of rigid transformations on 2D digital images, and models this space by a combinatorial structure, namely a graph. This structure presents a space complexity of  $\mathcal{O}(N^9)$  for any subset of  $\mathbb{Z}^2$  of size  $N \times N$ . Moreover, an algorithm to build this graph with *exact computation* (i.e., using only integers), in linear time with respect to its space complexity is proposed in [7].

### 2.2 Topology-preserving digital image transformations

The study of discrete deformations involving topological alteration, relies mostly – but not exclusively [22] – on the notion of simple point, which provides conditions for the preservation of strong topological invariants, and in particular the homotopy-type. Intuitively, a point is called simple if its value can be modified without changing the digital topology of the associated image.

Simple points were initially defined for binary images on  $\mathbb{Z}^2$  [23]. This notion was later formulated in the framework of digital topology [24], and was recently shown [25,26] to extend to richer discrete frameworks that explicitly describe cubic grids as topological spaces [27,28]. Several extensions have then been proposed during the following forty years, in terms of dimensions (3D [29] and 4D [30] simple points); of cardinality (deletable sets [31], P-simple points [32], minimal simple sets [33]); and in terms of image value spaces (grey-level images [34], label images [35–37]).

On the applicative front, simple points have been intensively used in the development of various pattern recognition methods, for instance in the field of medical image analysis [38]. In particular, many such methods have been defined in monotonic transformation paradigms [39] (*i.e.*, reduction, skeletonization, region-growing) or in – continuous [40] or discrete [36] – deformation model paradigms.

Only a few works have involved topology preservation notions combined with geometric transformations, for instance in the field of digital image warping [41,4] based on continuous deformation fields obtained from registration procedures. In particular, the question of digital topology preservation in the case of rigid transformations has – to the best of our knowledge – not been considered until now.

### 3 Background notions

#### 3.1 Digital images

In the continuous domain, a (2D) image can be formalised as a function  $\mathcal{I} : \mathbb{R}^2 \rightarrow \mathbb{V}$ , where  $\mathbb{V}$  is a value space. We assume that  $\mathbb{V}$  contains at least two elements, including one, noted  $\perp$ , corresponding to the “background” value. In particular:

- if  $|\mathbb{V}| = 2$ , then  $I$  is a binary image;
- if  $|\mathbb{V}| \geq 3$  and is equipped with a total order, then  $I$  is a grey-level image;
- if  $|\mathbb{V}| \geq 3$  and is not equipped with a total order, then  $I$  is a label image.

A (2D) *digital* image associated to  $\mathcal{I}$  can be defined as  $I : \mathbb{Z}^2 \rightarrow \mathbb{V}$ , by sampling  $\mathcal{I}$  on the discrete space  $\mathbb{Z}^2$ . In other words, we have  $I = \mathcal{I}|_{\mathbb{Z}^2}$ , and for each  $\mathbf{p} \in \mathbb{Z}^2$ , the value  $I(\mathbf{p})$  of the digital image models the value of  $\mathcal{I}$  on the associated pixel  $\mathbf{p} + [-\frac{1}{2}, \frac{1}{2}]^2$ , namely the Voronoi cell of  $\mathbb{R}^2$  induced by  $\mathbb{Z}^2$  around  $\mathbf{p}$ . This paradigm relies on the digitization function  $D$  defined as

$$\left| \begin{array}{l} D : \mathbb{R}^2 \longrightarrow \mathbb{Z}^2 \\ (x, y) \longmapsto ([x], [y]) \end{array} \right. \quad (1)$$

where  $[\cdot]$  is a standard rounding function (for instance, the floor function  $\mathbf{x} \rightarrow \lfloor \mathbf{x} + (\frac{1}{2}, \frac{1}{2}) \rfloor$ ). We assume that a digital image is actually defined on a subset of  $\mathbb{Z}^2$ , namely  $I^{-1}(\mathbb{V} \setminus \{\perp\})$ , which is finite. Then, it is plain that  $I^{-1}(\mathbb{V} \setminus \{\perp\}) \subseteq \mathbb{S} = [0, N-1]^2 \cap \mathbb{Z}^2$ , for a given  $N \in \mathbb{N}$ . The set  $\mathbb{S}$  is called the support of  $I$  and  $N \times N$  is the size of  $I$ . By abuse of notation – and without loss of generality – we will sometimes note a digital image as  $I : \mathbb{S} \rightarrow \mathbb{V}$  instead of  $I : \mathbb{Z}^2 \rightarrow \mathbb{V}$ .

#### 3.2 Digital rigid transformations

In the continuous framework, a rigid transformation (composed of translations and rotations) is expressed as a bijec-

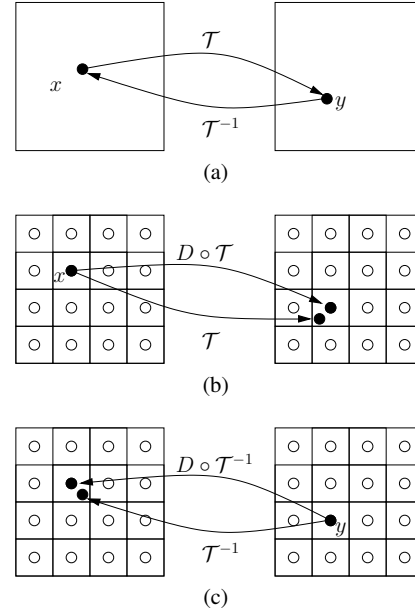


**Fig. 2** (a) Forwards and backwards transformation models in  $\mathbb{R}^2$ . (b) Lagrangian and (c) Eulerian transformation models in  $\mathbb{Z}^2$ .

tion  $\mathcal{T} : \mathbb{R}^2 \rightarrow \mathbb{R}^2$  defined, for any  $\mathbf{x} = (x, y) \in \mathbb{R}^2$  by

$$\mathcal{T}(\mathbf{x}) = \begin{pmatrix} \cos \theta & -\sin \theta \\ \sin \theta & \cos \theta \end{pmatrix} \begin{pmatrix} x \\ y \end{pmatrix} + \begin{pmatrix} a \\ b \end{pmatrix} \quad (2)$$

where  $a, b \in \mathbb{R}$  and  $\theta \in [0, 2\pi[$ . Such a transformation is unambiguously modeled by the triplet of parameters  $(a, b, \theta)$ , and will sometimes be noted  $\mathcal{T}_{ab\theta}$ .

It is not possible to apply directly  $\mathcal{T}$  on a digital image  $I : \mathbb{S} \rightarrow \mathbb{V}$ , since there is no guarantee that  $\mathcal{T}(\mathbf{x}) \in \mathbb{Z}^2$ , for any  $\mathbf{x} \in \mathbb{Z}^2$ . The correct handling of *digital* rigid transformations then requires to define a digital analogue  $T : \mathbb{Z}^2 \rightarrow \mathbb{Z}^2$  of  $\mathcal{T}$ . By considering the digitization paradigm proposed in Equation (1), this can be conveniently performed by setting

$$T = D \circ \mathcal{T}|_{\mathbb{S}} \quad (3)$$

In other words, the transformation  $T$  is obtained by applying  $\mathcal{T}$  and then digitising the result by the function  $D$ , as illustrated in the diagram below.

$$\begin{array}{ccc} \mathbb{S} \subseteq \mathbb{Z}^2 & \xrightarrow{T=D \circ \mathcal{T}|_{\mathbb{S}}} & T(\mathbb{S}) \subseteq \mathbb{Z}^2 \\ \downarrow Id & & \uparrow D \\ \mathbb{S} \subseteq \mathbb{R}^2 & \xrightarrow{\mathcal{T}} & \mathcal{T}(\mathbb{S}) \subseteq \mathbb{R}^2 \end{array} \quad (4)$$

The function  $T : \mathbb{Z}^2 \rightarrow \mathbb{Z}^2$  is then explicitly defined, for any  $\mathbf{p} = (p, q) \in \mathbb{Z}^2$ , by

$$T(\mathbf{p}) = D \circ \mathcal{T}(\mathbf{p}) = \begin{pmatrix} [p \cos \theta - q \sin \theta + a] \\ [p \sin \theta + q \cos \theta + b] \end{pmatrix} \quad (5)$$

In  $\mathbb{R}^2$ , the transformation  $\mathcal{T} : \mathbb{R}^2 \rightarrow \mathbb{R}^2$  is bijective. Consequently, determining  $\mathbf{y} \in \mathbb{R}^2$  such that  $\mathcal{T}(\mathbf{x}) = \mathbf{y}$ , and determining  $\mathbf{x} \in \mathbb{R}^2$  such that  $\mathcal{T}^{-1}(\mathbf{y}) = \mathbf{x}$ , are equivalent questions. The first issue corresponds to the forwards model for image transformation, while the second issue corresponds to the backwards model (Fig. 2(a)).

In general, the bijectivity hypothesis is no longer verified in the digital case, for  $T = D \circ \mathcal{T}_{\mathbb{S}} : \mathbb{Z}^2 \rightarrow \mathbb{Z}^2$ . In such a context, the forwards model (namely the Lagrangian model, illustrated in Fig. 2(b)) can be correctly handled, but not the backwards model (namely the Eulerian model). However, by setting  $T^{-1} = D \circ \mathcal{T}_{\mathbb{Z}^2}^{-1} : \mathbb{Z}^2 \rightarrow \mathbb{Z}^2$ , we can define a transformed digital image  $I \circ T^{-1} : \mathbb{Z}^2 \rightarrow \mathbb{V}$  that conveniently enables to handle the Eulerian model (Fig. 2(c)). (Note that  $T^{-1}$  is not the inverse function of  $T$  in general.)

In the sequel, we only focus on the Eulerian model (the justification of this choice will be discussed in Sec. 8). From this point on – for the sake of readability and without loss of correctness – we will note  $T$  instead of  $T^{-1}$ , due to the bijectivity of  $\mathcal{T}$  and  $\mathcal{T}^{-1}$ .

### 3.3 The topology of digital images

In the context of digital image transformations, the preservation of the image topology is often required, that is the preservation of given topological invariants. Among these topological invariants, the homotopy-type [42] is generally considered. As stated in Sec. 2.2, such homotopy-type preservation can be conveniently handled thanks to the notion of simple point, as described in the following property.

**Property 1 ([23])** *Let  $I : \mathbb{Z}^2 \rightarrow \mathbb{V}$  be a digital image. Let  $\mathbf{p} \in I$  be a simple point of  $I$ . Then, the modified image  $I'$ , obtained from  $I$  by modifying the value of  $I$  at  $\mathbf{p}$  into a licit value (depending on  $\mathbb{V}$  and  $I$ ) has the same homotopy-type as  $I$ .*

Some examples and counter-examples of simple points are provided in Fig. 3.

**Remark 2** *The notion of simplicity can be extended to sets of (successively) simple points between the initial image  $I$  and a final image  $I'$ , that still preserves the homotopy-type between  $I$  and  $I'$ . This leads to a notion of simple-equivalence [43] between images.*

Independently from the kind of topological structure [24, 27, 28] mapped on  $\mathbb{Z}^2$ , and from the value space  $\mathbb{V}$ , simple points have the virtue of being characterizable by considering their immediate neighbourhood.

**Property 3** *Let  $I : \mathbb{Z}^2 \rightarrow \mathbb{V}$  be a digital image. Let  $\mathbf{p} \in \mathbb{Z}^2$  be a point of  $I$ . The characterization of  $\mathbf{p}$  as a simple point can be computed locally and in constant time by only considering the points  $\mathbf{q} \in \mathbb{Z}^2$  such that  $\|\mathbf{p} - \mathbf{q}\|_{\infty} \leq 1$ .*

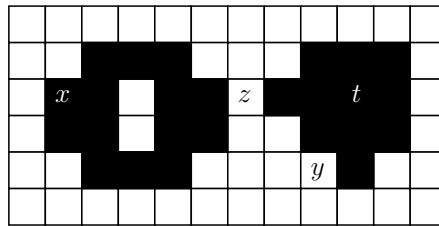


**Fig. 3** Examples of simple ( $\mathbf{x}, \mathbf{y}$ ) and non-simple ( $\mathbf{z}, \mathbf{t}$ ) points in a binary image. Modifying the value of  $\mathbf{z}$  would merge two black connected components, while modifying the value of  $\mathbf{t}$  would create a white connected component. In both cases, the homotopy-type of the image would be modified.

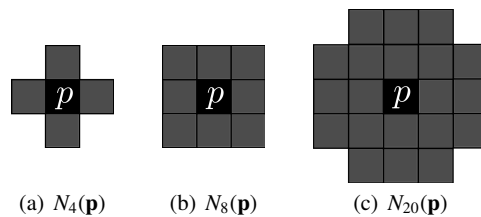


**Fig. 4** The neighbourhoods  $N_4$ ,  $N_8$  and  $N_{20}$  of a point  $\mathbf{p}$ .

Based on these considerations, the concepts developed in the sequel of this article require only the following two hypotheses related to the considered images  $I : \mathbb{Z}^2 \rightarrow \mathbb{V}$ :

- (H1)  $\mathbb{Z}^2$  is equipped with a standard topological structure [24, 27, 28]; and
- (H2) for this topological structure and the value space  $\mathbb{V}$ , a notion of simple point is available (this is, for instance, the case for binary, grey-level or label images).

For the sake of readability – but without loss of generality – we will hereafter focus on binary images endowed with the digital topology [24]. In this framework, the topological notions derive from a graph structure induced by two dual adjacency (*i.e.*, irreflexive and symmetric) relations, namely the 4- and 8-adjacencies, which are defined as follows. However, it is important to note that the results stated hereafter remain valid whenever hypotheses (H1) and (H2) are satisfied, as discussed in Sec. 6.3.

**Definition 4 ([24])** *Given a point  $\mathbf{p} = (p_1, p_2) \in \mathbb{Z}^2$ , we consider the two neighbourhoods  $N_4$  and  $N_8$ , which are defined for  $\mathbf{p}$  as sets of points  $\mathbf{q} = (q_1, q_2) \in \mathbb{Z}^2$  such that*

$$N_4(\mathbf{p}) = \{\mathbf{q} \in \mathbb{Z}^2 \mid \|\mathbf{p} - \mathbf{q}\|_1 = \sum_{i=1}^2 |p_i - q_i| \leq 1\} \quad (6)$$

$$N_8(\mathbf{p}) = \{\mathbf{q} \in \mathbb{Z}^2 \mid \|\mathbf{p} - \mathbf{q}\|_{\infty} = \max_{i=1}^2 |p_i - q_i| \leq 1\} \quad (7)$$

*We say that the point  $\mathbf{q}$  is 4- (resp. 8-) adjacent to  $\mathbf{p}$  if  $\mathbf{q} \in N_4(\mathbf{p}) \setminus \{\mathbf{p}\}$  (resp.  $\mathbf{q} \in N_8(\mathbf{p}) \setminus \{\mathbf{p}\}$ ).*

**Remark 5** *For reasons that will be justified in Sec. 6.1, we introduce a third neighbourhood for point  $\mathbf{p}$ , namely  $N_{20}$ , as*

well as the induced adjacency relation: the 20-adjacency. It is defined by

$$N_{20}(\mathbf{p}) = \left\{ \mathbf{q} \in \mathbb{Z}^2 \mid \|\mathbf{p} - \mathbf{q}\|_2 = \left( \sum_{i=1}^2 (p_i - q_i)^2 \right)^{1/2} < 2\sqrt{2} \right\} \quad (8)$$

From the adjacency relations induced by these neighbourhoods (illustrated in Fig. 4), we define the notion of paths and derive important topological concepts from connectedness to fundamental groups. In this framework, the characterization of simple points  $\mathbf{p}$  (which are either 4- or 8-simple, according to the chosen adjacency for the point value) can be made by only considering  $N_8(\mathbf{p})$  (see Property 3).

#### 4 Digital rigid transformations: Topological issues

As stated in Sec. 3.2, going from rigid transformations in  $\mathbb{R}^2$  (Equation (2)) to digital rigid transformations in  $\mathbb{Z}^2$  (Equation (5)) requires considering a digitization function (Equation (1)) that discretizes both the space and the transformation. In this section, we investigate such digitization effects on the topological properties of digital images during rigid transformations.

##### 4.1 Non-preservation of geometric properties

In  $\mathbb{R}^2$ , rigid transformations are isometries and so preserve distances (in particular the Euclidean distance) between any pair of points, as well as the angles induced by any triplet of (distinct) points. However, when rigid transformations are digitised from  $\mathbb{R}^2$  to  $\mathbb{Z}^2$ , these properties are often lost. Indeed, let us consider a point  $\mathbf{p} \in \mathbb{Z}^2$  and a point  $\mathbf{q} \in N_8(\mathbf{p}) \setminus \{\mathbf{p}\}$ . Let  $\mathbf{p}'$  and  $\mathbf{q}'$ , obtained from a digital rigid transformation of  $\mathbf{p}$  and  $\mathbf{q}$ , respectively. We have

$$d_2(\mathbf{p}, \mathbf{q}) = 1 \implies d_2(\mathbf{p}', \mathbf{q}') \in \{0, 1, \sqrt{2}\} \quad (9)$$

$$d_2(\mathbf{p}, \mathbf{q}) = \sqrt{2} \implies d_2(\mathbf{p}', \mathbf{q}') \in \{1, \sqrt{2}, 2\} \quad (10)$$

where  $d_2$  denotes the Euclidean distance. Similarly, alterations related to the angles between points can be derived as well.

**Remark 6** *The fact that we may have  $d_2(\mathbf{p}', \mathbf{q}') = 0$  when  $d_2(\mathbf{p}, \mathbf{q}) = 1$  also implies that digital rigid transformations are non-injective in general. Due to the discrete nature of  $\mathbb{Z}^2$ , this also implies that such transformations are non-surjective.*

We show, in the remainder of this section, how such alterations can raise topological issues in the transformed spaces. To this end, we will first study some properties of pixels related to the influence of digital rigid transformations on their neighbourhoods.

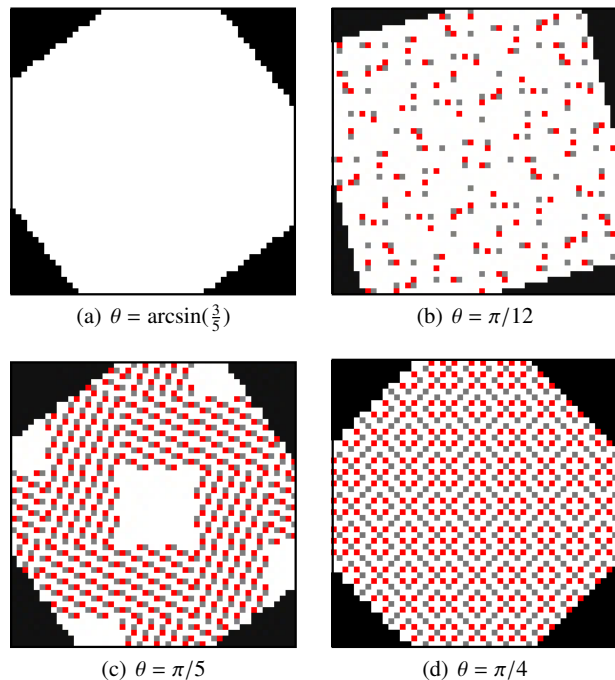


**Fig. 5** Some digital rotations by angles  $\theta$  of a white square of size  $100 \times 100$ . Double points are depicted in red, and null points in grey.

##### 4.2 Topological alterations due to digitization

From Remark 6, a digital rigid transformation  $T$  is generally not bijective. It is plain that for any three distinct points  $\mathbf{p}_1, \mathbf{p}_2, \mathbf{p}_3 \in \mathbb{Z}^2$ , we have  $\max_{i,j \in \{1,2,3\}} \{d_2(\mathbf{p}_i, \mathbf{p}_j)\} \geq \sqrt{2}$ . From Equation (10), we derive that the three points  $\mathbf{p}'_1, \mathbf{p}'_2, \mathbf{p}'_3$  obtained by a digital rigid transformation  $T$  of  $\mathbf{p}_1, \mathbf{p}_2, \mathbf{p}_3$  can not be mapped into the same pixel by the associated rigid transformation  $\mathcal{T}$ . It follows that we can characterise the *status* of a point  $\mathbf{p} \in \mathbb{Z}^2$  with respect to  $T$  by using the set  $P_T(\mathbf{p}) = \{\mathbf{q} \in \mathbb{Z}^2 \mid T(\mathbf{q}) = \mathbf{p}\}$  containing all points  $\mathbf{q} \in \mathbb{Z}^2$  whose images by  $T$  is  $\mathbf{p}$ . In particular, there exist only three possibilities.

**Definition 7** *Let us consider a point  $\mathbf{p} \in \mathbb{Z}^2$ , and a digital rigid transformation  $T$ .*

- If  $|P_T(\mathbf{p})| = 0$ , then  $\mathbf{p}$  is called a null point.
- If  $|P_T(\mathbf{p})| = 1$ , then  $\mathbf{p}$  is called a single point.
- If  $|P_T(\mathbf{p})| = 2$ , then  $\mathbf{p}$  is called a double point.

From Definition 7, a digital rigid transformation  $T$  behaves like a bijection for single points, while the possible existence of null and double ones generally forbids  $T$  to be a surjection and an injection, as already evoked in Remark 6. This is a well-known issue, which has already been identified in the literature dealing with rotations in discrete spaces, for instance [8, 44, 19, 21, 45]. Some examples are provided in Fig. 5.

The existence of null and double points is a major source of topological alterations. Indeed, some connected compo-

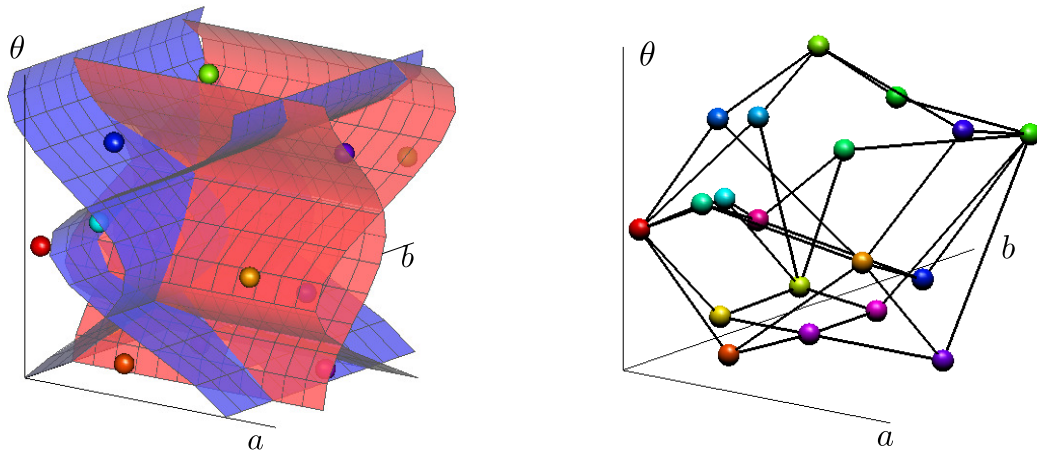


**Fig. 6** A part of the parameter space subdivided by four 2D surfaces bounding the DRTs (left), and the associated (part of the) DRT graph (right).

nents may be lost when applying a digital rigid transformation, in particular the one-pixel components.

In addition to such cardinality-based problems, some adjacency-based issues are derived from the geometric alterations evoked in Sec. 4.1. Indeed, the non-preservation of distances between points, when applying a digital rigid transformation, has a direct interpretation in terms of modification of the adjacency relations between such points. The adjacency relations between points may change from 4- to 8-adjacency or *vice versa*, or could even lead to a loss of adjacency between points initially 8-adjacent. In such situations, some connected components may be either split or merged.

**Remark 8** *Some topological alterations of the discrete structure of a subset  $\mathbb{S}$  of  $\mathbb{Z}^2$  do not necessarily lead to topological modifications of an image  $I$  defined on  $\mathbb{S}$ . Consequently, the study of the potential topological alterations induced by digital rigid transformations must be considered not only as a transformation-dependent problem, but also as an image-dependent one.*

## 5 DRT graphs and image topology

In this section, we briefly recall the notion of DRT graph proposed in [7], which is used to model the subdivision of the parameter space  $(a, b, \theta)$  of rigid transformations. Then, we discuss how to use this structure as a topological analysis tool for rigidly transformed images.

### 5.1 A brief presentation of the DRT graph

Contrarily to rigid transformations in  $\mathbb{R}^2$  (see Equation (2)), *digital rigid transformations* are not continuously defined

with respect to the parameters  $a, b$  (controlling the “translation” part) and  $\theta$  (controlling the “rotation” part). More precisely, the parameter space  $\mathbb{R}^3$  of  $(a, b, \theta)$  is divided into 3D open cells, in which the transformations  $T_{ab\theta}$  are equal, while the 2D surfaces bounding these open cells correspond to discontinuities of the digital rigid transformations, induced by the digitization process (see Equation (5)).

From a theoretical point of view, each 3D open cell of the parameter space  $(a, b, \theta)$  can be seen as an equivalence class of rigid transformations  $\mathcal{T}$  of  $\mathbb{R}^2$  that lead to a same transformation  $T = D \circ \mathcal{T}$  in  $\mathbb{Z}^2$ . Such an equivalence class is called a *discrete rigid transformation*<sup>1</sup> (DRT) [7]. Each 3D open cell can also be considered as the resulting digital transformed space generated by any digital rigid transformation of the associated DRT. Moreover, the existence of a 2D surface between two cells indicates that the two associated transformed images differ by exactly one pixel. By mapping any 3D cell onto a 0D point, and any 2D surface onto a 1D edge, the combinatorial structure of the parameter space can be modeled, in a dual way, as a (connected) graph, namely a *DRT graph* (see Fig. 6).

**Definition 9** ([7]) *Let  $G = (V, E)$  be the graph defined such that:*

- any vertex  $v \in V$  models a 3D open cell associated to a DRT;
- any edge  $e = (v, w) \in E$  models a 2D surface between two distinct vertices  $v, w \in V$ .

*The graph  $G = (V, E)$  is called a DRT graph.*

A DRT graph models the subdivision of the whole rigid transformation parameter space; therefore, it models *all* the

<sup>1</sup> The term *digital* refers to the digitization process of numeric images and transformations for such images, while the term *discrete* refers to the non-continuous structure of these transformations.



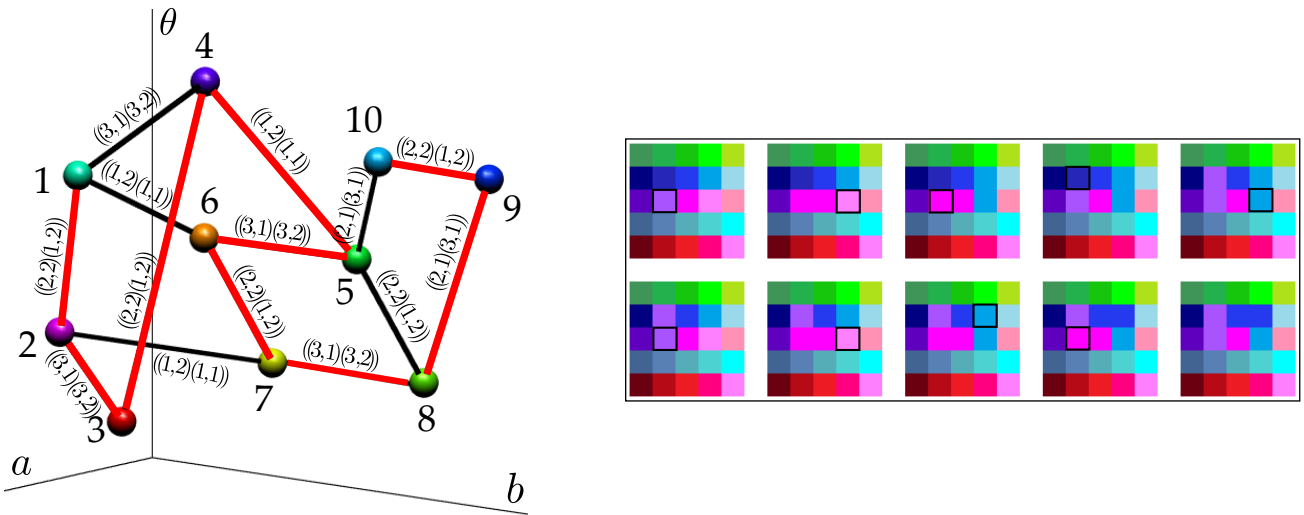


**Fig. 7** Left: part of a DRT graph  $G$  in which each vertex is a DRT representing a digital transformed image, and each edge indicates the *only* value modification of a pixel between two connected vertices. More precisely, if an edge  $e = (v, w, (\mathbf{p}, \mathbf{p}'))$  connects two vertices  $v$  and  $w$ , then the associated images  $I_v$  and  $I_w$  of  $v$  and  $w$  differ at the *single* pixel  $\mathbf{p}'$ , and  $\mathbf{p}$  is the pixel corresponding to  $\mathbf{p}'$  in the original image (see text). Right: the transformed images associated to the vertices of the DRT graph  $G$  and their relations according to the edges in  $G$ . The images from left to right and from top to bottom correspond to the path from the vertices 1 to 10 (in red), in which the differing pixel  $\mathbf{p}'$  between two transformed images of the consecutive vertices  $I_{v_i}$  and  $I_{v_{i+1}}$  is depicted by the black frame in  $I_{v_i}$ , and the first image corresponds to the original image.

possible rigid transformations of a given set  $\mathbb{S}$ . Despite the fact that the space of these transformations is infinite, the DRT graph is actually defined as a *finite* structure. In [7], the space complexity of the DRT graph for any set  $\mathbb{S}$  of size  $N \times N$  has been proved to be polynomial. An exact computation algorithm also exists to build this graph in linear time with respect to its size.

**Property 10 ([7])** *The DRT graph associated to a set  $\mathbb{S}$  of size  $N \times N$  has a space complexity of  $O(N^9)$ .*

DRT graphs do not depend on the values that are assigned to the pixels of  $\mathbb{S}$ . In other words, their structure is invariant for any image defined on a same support  $\mathbb{S}$ . In the sequel, we will however consider – without loss of generality – a DRT graph with respect to a given image  $I$  defined on  $\mathbb{S}$ . In this context, any edge  $e = (v, w) \in E$  of the DRT graph can be “enriched” as  $e = (v, w, (\mathbf{p}, \mathbf{p}'))$ , where  $\mathbf{p}'$  is the only pixel where the transformed images differ with respect to the DRTs  $v$  and  $w$ , respectively, while  $\mathbf{p}$  is the pixel corresponding to  $\mathbf{p}'$  in the initial image  $I$ .

The DRT graph relies on geometric information provided by  $(a, b, \theta)$ . However, it does not explicitly model such geometric information. Indeed, it only provides structural information, that models the relationship between any “neighbouring” transformed images. In particular, the label  $(\mathbf{p}, \mathbf{p}')$  of each edge  $e$  is implicitly associated to a function indicating the value modification of the pixel  $\mathbf{p}'$  that differs between the transformed images corresponding to the DRTs  $v$  and  $w$ . More precisely, the rigid transformation associated to the 2D surface of the edge  $e$  modifies only the pixel value of  $\mathbf{p}'$  (which is initially equal to the value of  $\mathbf{p}$ ), such that  $\mathbf{p}'$

will get its value from one of the 4-neighbouring pixels of  $\mathbf{p}$ . This property is exemplified in Fig. 7. Practically, let  $I_v$  and  $I_w$  be the transformed images corresponding to the vertices  $v$  and  $w$  respectively. The value of  $\mathbf{p}'$  at the vertex  $v$  is defined by  $I_v(\mathbf{p}') = I(\mathbf{p})$  where  $I : \mathbb{S} \rightarrow \mathbb{V}$  is the original image function. After the elementary modification at the edge  $e$ , we obtain a new transformed image  $I_w$  by simply changing the pixel value at  $\mathbf{p}'$  as  $I_w(\mathbf{p}') = I(\mathbf{p} + \delta)$  where  $\delta = (\pm 1, 0)$  or  $(0, \pm 1)$ . In this way, one can generate all the transformed images of  $I$  by incrementally and exhaustively scanning the associated DRT graph.

**Remark 11** *Let  $G = (V, E)$  be a DRT graph associated to a given image  $I : \mathbb{S} \rightarrow \mathbb{V}$ . For each edge  $e = (v, w, (\mathbf{p}, \mathbf{p}')) \in E$ , two cases can occur:*

- (i)  $I_v(\mathbf{p}') = I_w(\mathbf{p}')$ , i.e., the transformed images of  $I$  by the DRTs  $v$  and  $w$  are equivalent ( $I_v = I_w$ );
- (ii)  $I_v(\mathbf{p}') \neq I_w(\mathbf{p}')$ , i.e.,  $I_v \neq I_w$ .

In the case of binary images, the value of  $\mathbf{p}'$  may then be flipped from white to black or *vice versa*, and this may constitute the only modification between the images of  $I$  by two consecutive DRTs. Such a value change may consequently alter the topological property of the binary images. In the sequel, we will show how to verify whether this actually occurs, for any arbitrary transformations, using a DRT graph.

## 5.2 DRT graph as a topological analysis tool

On the one hand, we would like to know if a given image  $I$  defined on  $\mathbb{S}$  preserves its topological properties under all



digital/discrete rigid transformations. Let us first formalise this preservation, via the notion of *topological invariance*.

**Definition 12** A digital image  $I$  is topologically invariant if all its transformed images have the same homotopy-type as  $I$ .

On the other hand, as mentioned in Sec. 5.1 the DRT graph allows us to generate exhaustively *all* the transformed images of  $I$ . From the definition of the DRT graph and from Remark 11, this can be achieved by incrementally modifying (at most) one pixel value between two successive transformed images. Moreover, from Property 1, the notion of simple point can be used to handle the topological-invariance concept (in particular, the homotopy-type) between two images that differ in exactly one point. We also know from Remark 2 that this preservation of the homotopy-type is also guaranteed via the notion of simple-equivalence, that consists of considering successively simple points. The local characterization of simple points and the incremental notion of simple-equivalence are therefore compatible with an incremental exploration of the DRT graph of image  $I$ , in order to evaluate its topological invariance.

Practically, the edges of the DRT graph  $G = (V, E)$  of  $I$  can be classified in two categories: those that do not modify the topology of the transformed images and those that do. The first category contains the edges that correspond to the case (i) in Remark 11 as well as those that correspond to the case (ii) for which  $\mathbf{p}'$  is a simple point; and the second one contains the edges that correspond to the case (ii) in Remark 11 for which  $\mathbf{p}'$  is not simple.

Based on this binary classification, we can straightforwardly create a partial graph  $G' = (V, E')$  of  $G$  by preserving in  $E' \subseteq E$  only the edges of the first category. In particular, if  $G'$  is connected, it is plain that  $I$  is topologically invariant. Otherwise,  $I$  is not topologically invariant, and every connected component in  $G'$  corresponds to a set of simple-equivalent transformed images. It should be noticed that if there exist at least 3 such connected components, there is no guarantee of maximality of this simple-equivalence property. In other words, two separate (and non-adjacent) connected components in  $G'$  may be composed of images that all present the same topology. This property derives from the fact that the DRT graph does not model all the possible paths associated to transformations between two images, but is restricted to those that have a rigid transformation semantics.

Such an approach presents an algorithmic complexity that is linear with respect to the (polynomial) space complexity of the DRT graph. It is however possible to reach a better (mean) complexity by using a standard spanning-tree algorithm (see Algorithm 1), that provides two outputs: a Boolean evaluating the topological invariance of  $I$ , and a (non-necessarily maximal) set of simple-equivalent transformed images with respect to the image associated to the

---

**Algorithm 1:** Generation of simple-equivalent images and topological invariance verification.

---

**Input:** A DRT graph  $G = (V, E)$  associated to an image  $I$ .  
**Input:** An initial vertex  $u \in V$  corresponding to the image  $I$ .  
**Output:** A partial sub-graph  $G'' = (V'', E'')$  of  $G$  such that, for any  $v \in V''$ , the images  $I_v$  are simple-equivalent to  $I$ .  
**Output:** A Boolean  $B$  that indicates if  $I$  is a topologically invariant image.

```

1  $(V'', E'') \leftarrow (\{u\}, \emptyset)$ 
2  $S \leftarrow \{u\}$ 
3 while  $S \neq \emptyset$  do
4   Let  $v \in S$ 
5    $S \leftarrow S \setminus \{v\}$ 
6   foreach  $e = (v, w, (\mathbf{p}, \mathbf{p}')) \in E$ , such that  $w \notin V''$  do
7     if  $(I_v(\mathbf{p}') = I_w(\mathbf{p}'))$  or  $((I_v(\mathbf{p}') \neq I_w(\mathbf{p}'))$  and  $(\mathbf{p}'$  is a
8       simple point in  $I_v)$  then
9          $(V'', E'') \leftarrow (V'' \cup \{w\}, E'' \cup \{e\})$ 
           $S \leftarrow S \cup \{w\}$ 
10  $B \leftarrow (V = V'')$ 

```

---

initial vertex  $u$  in the DRT graph (e.g.,  $I$  or any other transformed image of  $I$ ). In Algorithm 1, the graph  $G''$  providing the set of simple-equivalent images is in fact a partial sub-graph of  $G'$  (and of  $G$  as well).

Nevertheless, the high algorithmic complexity of this approach practically forbids the generation the whole graph for large images, and therefore to consequently verify topological invariance. In the next section, we show that this problem can however be decomposed spatially, thus leading to a much lower complexity algorithm.

## 6 A local approach for analyzing topological invariance under DRTs

In the previous section, we have proposed to explore the whole DRT graph of a given image  $I$  in order to evaluate its topological invariance for all DRTs. More precisely, for each edge  $e = (v, w, (\mathbf{p}, \mathbf{p}'))$  of the DRT graph, this exploration consists of verifying that  $\mathbf{p}'$  is a simple point between the transformed images  $I_v$  and  $I_w$  with respect to the DRTs  $v$  and  $w$ , if  $I_v \neq I_w$ . From Property 3, we know that this verification can be carried out locally, more precisely in the neighbourhood  $N_8(\mathbf{p}')$  of the transformed image space(s). We now propose to take advantage of the local nature of these tests to develop a space decomposition strategy that leads to a *local* version of the previously proposed *global* method.

### 6.1 From global to local DRTs

On the one hand, it is plain that the set of all DRTs defined on a subset of size  $N \times N$  of  $\mathbb{Z}^2$ , does not depend on the way to locate this subset into  $\mathbb{Z}^2$ . In other words – provided that

we choose a set  $\mathbb{S} \subset \mathbb{Z}^2$  “sufficiently large” to include the informative part of  $I$  – the DRT graph  $G = (V, E)$  associated to an image  $I : \mathbb{S} \rightarrow \mathbb{V}$  is isomorphic to the DRT graph of any translated image of  $I$  (this isomorphism actually concerns the vertices/edges that involve at least one point with a value distinct from  $\perp$ ). In particular, for a given  $\mathbf{p} \in \mathbb{Z}^2$  let us consider the image  $I_{\mathbf{p}}$  such that for any  $\mathbf{q} \in \mathbb{Z}^2$ ,  $I_{\mathbf{p}}(\mathbf{q}) = I(\mathbf{q} - \mathbf{p})$ . Then, any edge  $e = (v, w, (\mathbf{p}, \mathbf{p}'))$  of the DRT graph  $G$  of  $I$  is equivalent to the edge  $e' = (v', w', (\mathbf{0}, \mathbf{p}'))$  (also denoted by  $e' = (v', w', (\mathbf{o}_1, \mathbf{p}'))$  in the following) of the DRT graph  $G_{\mathbf{p}}$  of  $I_{\mathbf{p}}$  and  $v', w'$  are the DRTs corresponding to  $v, w$ , respectively, up to the translation of vector  $-\mathbf{p}$ .

On the other hand, let us consider an edge  $e = (v, w, (\mathbf{p}, \mathbf{p}'))$  of the DRT graph  $G$  of  $I$ . For a given  $\mathbf{p}' \in \mathbb{Z}^2$ , we can have two images  $I_{v'}$  and  $I_{w'}$  with respect to  $I_v$  and  $I_w$  such that, for any  $\mathbf{q} \in \mathbb{Z}^2$ ,  $I_{v'}(\mathbf{q}) = I_v(\mathbf{q} - \mathbf{p}')$  and  $I_{w'}(\mathbf{q}) = I_w(\mathbf{q} - \mathbf{p}')$ . Therefore, any edge  $e = (v, w, (\mathbf{p}, \mathbf{p}'))$  is considered to be equivalent to  $e' = (v', w', (\mathbf{p}, \mathbf{0}))$  (also denoted by  $e' = (v', w', (\mathbf{p}, \mathbf{o}_2))$  in the following), where  $v', w'$  correspond to  $v, w$ , respectively, up to the translation of vector  $-\mathbf{p}'$ .

From the two above paragraphs, we derive the following statement.

**Remark 13** *The study of any edge of label  $(\mathbf{p}, \mathbf{p}')$  in the DRT graph  $G = (V, E)$  associated to an image  $I : \mathbb{S} \rightarrow \mathbb{V}$  can be carried out by considering the edge of label  $(\mathbf{o}_1, \mathbf{o}_2)$  in the equivalent DRT graph  $G_{\mathbf{p}} = (V_{\mathbf{p}}, E_{\mathbf{p}})$  associated to a translated image  $I_{\mathbf{p}}$  of  $I$ .*

In order to establish our local strategy, we now state some lemmas related to the behaviour of DRTs with respect to the 8-neighbourhood. Our first lemma, derived from Definition 4 and Equation (5), deals with the extension of a 8-neighbourhood induced by digital rigid transformations.

**Lemma 14** *Let  $\mathbf{p} \in \mathbb{Z}^2$  and  $\mathbf{q} \in N_8(\mathbf{p})$ . For any digital rigid transformation  $T : \mathbb{Z}^2 \rightarrow \mathbb{Z}^2$ , we have  $T(\mathbf{q}) \in N_{20}(T(\mathbf{p}))$ .*

From the result of Remark 13 and the local characterization of simple points (Property 3), we then derive the following lemma where we consider  $T_v$  as the digital rigid transformation associated to a DRT  $v$ , thanks to Lemma 14. Our next lemma states that it is sufficient to consider a local neighbourhood to evaluate simple points under rigid transformations.

**Lemma 15** *Let  $I : \mathbb{S} \rightarrow \mathbb{V}$  be a digital image. Let  $I' : N_{20}(\mathbf{p}) \rightarrow \mathbb{V}$  be the restriction of  $I$  to  $N_{20}(\mathbf{p})$  for any  $\mathbf{p} \in \mathbb{S}$ . Let  $v, w$  (resp.  $v', w'$ ) be two adjacent vertices of the DRT graph  $G$  (resp.  $G'_{\mathbf{p}}$ ) associated to  $I$  (resp.  $I'$ ) such that the DRTs  $T_v, T_w$  (resp.  $T_{v'}, T_{w'}$ ) differ only in  $\mathbf{p}'$  and  $T_v(\mathbf{p}') = \mathbf{p}$  (resp.  $T_{v'}(\mathbf{p}') = \mathbf{p}$ ). Let  $I_v, I_w : \mathbb{S} \rightarrow \mathbb{V}$  (resp.  $I_{v'}, I_{w'} : N_{20}(\mathbf{p}) \rightarrow \mathbb{V}$ ) be the transformed images of  $I$  (resp.  $I'$ ) with respect to  $v, w$  (resp.  $v', w'$ ), according to the Eulerian model. Then  $\mathbf{p}'$  is a simple point in  $I_v$  (and  $I_w$ ) iff  $\mathbf{p}'$  is a simple point in  $I_{v'}$  (and  $I_{w'}$ ).*

In the DRT graph  $G$  of an image  $I$ , we can define an *equivalence relation* between the edges of  $G$  as follows.

**Definition 16** *Let  $G = (V, E)$  be the DRT graph associated to an image  $I$ , and  $E_{(\mathbf{p}, \mathbf{p}')} \subset E$  be the set of edges with  $(\mathbf{p}, \mathbf{p}')$  as their label. Two edges  $e_1 = (v_1, w_1, (\mathbf{p}, \mathbf{p}'))$  and  $e_2 = (v_2, w_2, (\mathbf{p}, \mathbf{p}'))$  in  $E_{(\mathbf{p}, \mathbf{p}')}$  are equivalent, and denoted by  $e_1 \sim e_2$ , iff  $T_{v_1 | N_8(\mathbf{p}')} = T_{v_2 | N_8(\mathbf{p}')}$  (and  $T_{w_1 | N_8(\mathbf{p}')} = T_{w_2 | N_8(\mathbf{p}')}$ ).*

In other words, an equivalence class of any  $e = (v, w, (\mathbf{p}, \mathbf{p}')) \in E_{(\mathbf{p}, \mathbf{p}')}$  under  $\sim$ , denoted by  $[(v, w, (\mathbf{p}, \mathbf{p}'))]_{\sim}$ , contains the set of  $T_v$  that provide the same transformed image in the restriction of  $I$  to  $N_{20}(\mathbf{p})$ . Let us consider the DRT graph  $G'_{\mathbf{p}}$  associated to the 20-neighbourhood of  $\mathbf{o}_1$  in the translated image  $I_{\mathbf{p}}$ . According to the Eulerian model and Lemma 14, this DRT graph  $G'_{\mathbf{p}}$  contains edges  $(v', w', (\mathbf{o}_1, \mathbf{o}_2))$  that “summarize” the edges  $(v, w, (\mathbf{p}, \mathbf{p}'))$  of the DRT graph  $G$  associated to  $I$ .

**Proposition 17** *Let  $E_{(\mathbf{p}, \mathbf{p}')} (resp. E'_{\mathbf{p}}(\mathbf{o}_1, \mathbf{o}_2))$  be the set of edges with  $(\mathbf{p}, \mathbf{p}')$  (resp.  $(\mathbf{o}_1, \mathbf{o}_2)$ ) as their label of the graph  $G = (V, E)$  (resp.  $G'_{\mathbf{p}} = (V'_{\mathbf{p}}, E'_{\mathbf{p}})$ ) associated to  $I$  (resp.  $I'_{\mathbf{p}}$ , the restriction of  $I_{\mathbf{p}}$  to  $N_{20}(\mathbf{o}_1)$ ). We have  $E_{(\mathbf{p}, \mathbf{p}')} / \sim$  equivalent to  $E'_{\mathbf{p}}(\mathbf{o}_1, \mathbf{o}_2)$ , by associating each equivalence class  $[(v, w, (\mathbf{p}, \mathbf{p}'))]_{\sim} \in E$  to the edge  $(v', w', (\mathbf{o}_1, \mathbf{o}_2)) \in E'_{\mathbf{p}}(\mathbf{o}_1, \mathbf{o}_2)$  such that  $T_v | N_8(\mathbf{p}') = T_{v'}$  and  $T_w | N_8(\mathbf{p}') = T_{w'}$ .*

Since  $\mathbf{o}_1$  and  $\mathbf{o}_2$  are the origins  $\mathbf{0}$  of the images  $I$  and  $I'_{\mathbf{p}}$  respectively, the relations between  $I, G, E_{(\mathbf{0}, \mathbf{0})}$  and  $I'_{\mathbf{p}}, G'_{\mathbf{p}}, E'_{\mathbf{p}}(\mathbf{0}, \mathbf{0})$  are illustrated in Figs. 8 and 9.

Based on Lemma 15 and Proposition 17, it follows that the “topological” behaviour of any edge of  $[(v, w, (\mathbf{p}, \mathbf{p}'))]_{\sim}$  in the DRT graph  $G$  associated to image  $I$  can be determined from the edges  $(v', w', (\mathbf{o}_1, \mathbf{o}_2))$  in the DRT graph  $G'_{\mathbf{p}}$ . In other words, the study of the *local* DRT graph  $G'_{\mathbf{p}}$  associated to the partial images of  $I$  defined on  $N_{20}(\mathbf{p})$  directly provides access to a subset of the required *global* knowledge related to the topological invariance of  $I$  under any DRTs.

In particular, from Remark 13, Lemmas 14, 15, and Proposition 17, it becomes possible to develop a local approach for the topological invariance verification of digital images under all rigid transformations.

## 6.2 LUT-based algorithm

Practically, an image  $I$  is topologically invariant with respect to all DRTs if all its transformed images share the same homotopy-type, and in particular if they are simple-equivalent (Remark 2). This simple-equivalence can be locally determined using the notion of simple point (Properties 1 and 3). In particular, any elementary modification between transformed images is encoded in an edge of the DRT graph  $G$  of  $I$ , and such an edge models the modification of exactly one point between two transformed images.

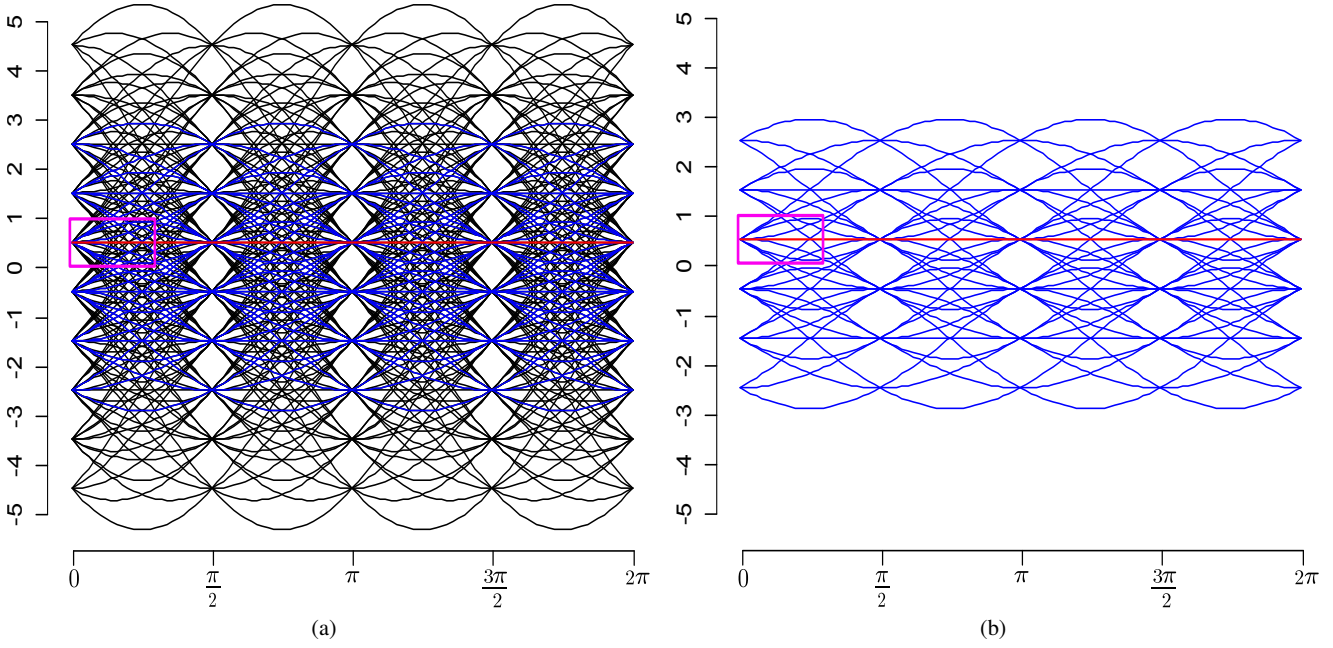


**Fig. 8** (a) A cross-section in the plane  $(a, \theta)$  of the 2D surfaces bounding the DRTs (see Sec. 5.1) associated to the image  $I$ , and inducing the DRT graph  $G = (V, E)$ . (b) A cross-section in the plane  $(a, \theta)$  of the 2D surfaces bounding DRTs associated to  $I' = I_{|N_{20}(\mathbf{0})}$ , and inducing the DRT graph  $G' = (V', E')$  (see text). In both figures, the red segments correspond to the edges of label  $(\mathbf{0}, \mathbf{0})$  (i.e.,  $E_{(\mathbf{0}, \mathbf{0})}$  and  $E'_{(\mathbf{0}, \mathbf{0})}$ ), while the blue ones are the edges in  $E'$  and the black ones are the edges in  $E \setminus E'$ .

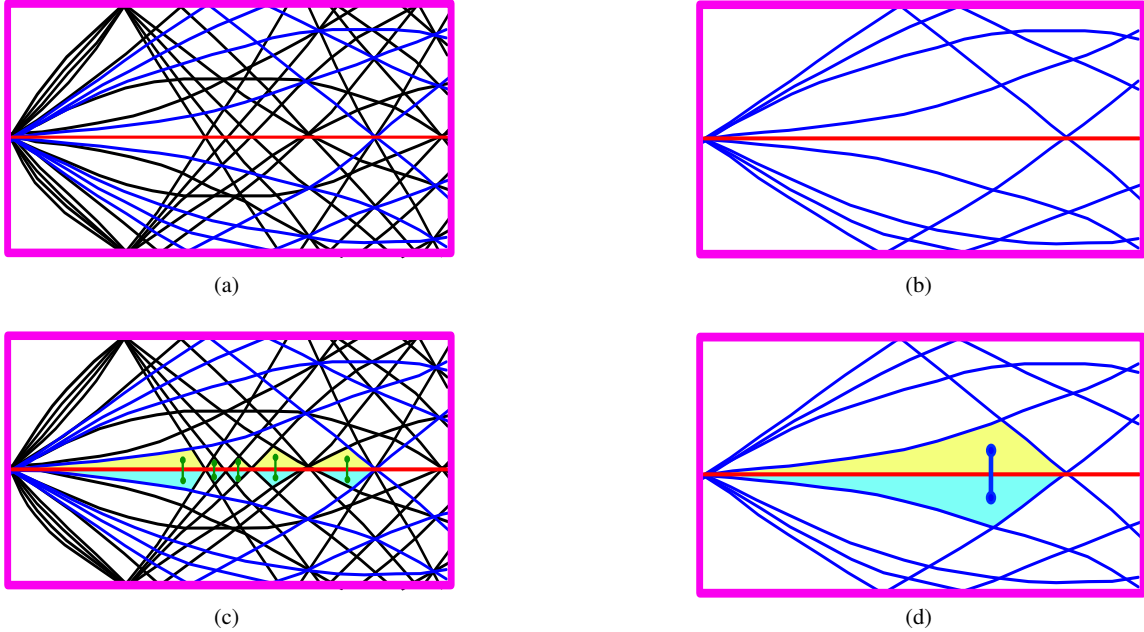


**Fig. 9** (a,b) Zoom in the curves of Fig. 8. (c,d) Illustration of the dual structures of (a,b) for the part of the DRT graph corresponding to the edges with label  $(\mathbf{0}, \mathbf{0})$ . By Definition 16, the green edges in (c) form an equivalence class  $[(v, w, (\mathbf{0}, \mathbf{0}))]_- \in E$ . From Proposition 17, the equivalence class  $[(v, w, (\mathbf{0}, \mathbf{0}))]_-$  can be associated to the blue edge  $(v', w', (\mathbf{0}, \mathbf{0}))$  in (d).

This point can in particular be characterised as simple or not. Consequently, by analysing the edges of the whole DRT graph  $G$ , the topological invariance of  $I$  can be determined. This is the strategy developed in Algorithm 1, that processes

these edges in an exhaustive fashion, leading to a computational cost directly linked to the size of the DRT graph.

In the previous section, it was observed that any edge of the DRT graph  $G$  of  $I : \mathbb{S} \rightarrow \mathbb{V}$  is equivalent to an edge in a smaller DRT graph  $G'_p$ , associated to the restriction of  $I$  in

---

**Algorithm 2:** LUT generation for topological invariance verification.

---

**Input:** The DRT graph  $G'_0 = (V'_0, E'_0)$  associated to  $N_{20}(\mathbf{0})$ .

**Input:** The set  $C$  of all different images  $I : N_{20}(\mathbf{0}) \rightarrow \mathbb{V}$  (computed in a greedy fashion).

**Output:** The set  $P \subseteq C$  of topologically preserving samples for the center point  $\mathbf{0}$ .

```

1  $P \leftarrow \emptyset$ 
2 foreach  $I \in C$  do
3    $B \leftarrow true$ 
4    $S \leftarrow E_0$ 
5   while ( $S \neq \emptyset$ ) and ( $B = true$ ) do
6     Let  $e = (v, w, (\mathbf{p}, \mathbf{p}')) \in S$ 
7      $S \leftarrow S \setminus \{e\}$ 
8     if  $\mathbf{p} = \mathbf{0}$  then
9       if ( $(I_v(\mathbf{p}')) \neq I_w(\mathbf{p}')$ ) and ( $\mathbf{p}'$  is not a simple point
10        in  $I_v$ ) then
11           $B \leftarrow false$ 
12   if  $B = true$  then
13      $P \leftarrow P \cup \{I\}$ 

```

---



---

**Algorithm 3:** Local verification of the topological invariance of a digital image.

---

**Input:** A digital image  $I : \mathbb{S} \rightarrow \mathbb{V}$ .

**Input:** The set  $P$  (computed from Algorithm 2).

**Output:** A Boolean value  $B$  evaluating the topological invariance of  $I$ .

```

1  $B \leftarrow true$ 
2  $S \leftarrow \mathbb{S}$ 
3 while ( $S \neq \emptyset$ ) and ( $B = true$ ) do
4   Let  $p \in S$ 
5    $S \leftarrow S \setminus \{p\}$ 
6    $B \leftarrow (I_{|N_{20}(\mathbf{p})} \in P)$  (up to a translation of  $-\mathbf{p}$ )

```

---

the 20-neighbourhood of a given point  $\mathbf{p} \in \mathbb{S}$  (Remark 13 and Proposition 17). In particular, the characterization of this edge as topologically preserving is algorithmically the same in  $G$  and in  $G'_p$  (Lemma 15 and Proposition 17).

From these facts, we deduce that the topological invariance of  $I$  can be equivalently analyzed from  $G$  or from the set  $\{G'_p\}_{p \in \mathbb{S}}$  of all the local DRT graphs in the 20-neighbourhoods of the points  $\mathbf{p} \in \mathbb{S}$ . In particular, in any of these local DRT graphs  $G'_p$ , it is sufficient to focus on a (strict) subset of edges, namely those that involve  $\mathbf{p}$ .

Moreover, since only a finite number of images can be defined on a 20-neighbourhood, this topological analysis can be performed exhaustively just once for all the images defined on a 20-neighbourhood; these images can then be used to characterize the topological invariance of  $I$ . This pre-computation, formalised in Algorithm 2, leads to the definition of a look-up table (LUT)  $P$  that contains all the 20-neighbourhood images that authorize topological invariance in a larger image, for a given value space  $\mathbb{V}$ , and a given topology.

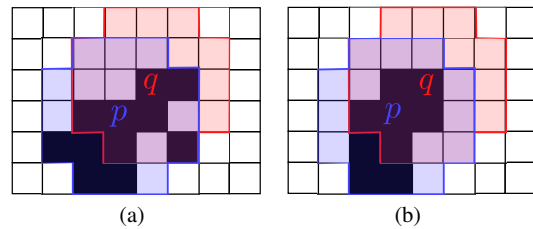


**Fig. 10** (a) A 20-neighbourhood image, centered on  $\mathbf{p}$  (in blue), that belongs to the LUT  $P$ , and an (overlapped) image, centered on  $\mathbf{q}$  (in red), that does not belong to  $P$ . (b) Two 20-neighbourhood images, centered on  $\mathbf{p}$  and  $\mathbf{q}$ , respectively, that both belong to the LUT  $P$ . (See Remark 18.)

**Remark 18** The LUT  $P$  obtained from Algorithm 2 potentially constitutes a strict superset of the actual set of the 20-neighbourhood images that authorize in the LUT some patterns that necessarily imply the existence of neighbouring patterns that are not themselves in the LUT (see Fig. 10). Algorithm 2 can then be optimised by a post-processing that removes from  $P$  some non-relevant configurations. Such a post-processing, that leads to a smaller LUT, presents a time complexity  $O(|P|^3)$ .

We discuss in more details experimental results obtained with this LUT in the case of binary images in Sec. 7.2. Once the LUT  $P$  has been computed, any image  $I : \mathbb{S} \rightarrow \mathbb{V}$  can be characterized by a simple pixelwise process, that checks, for every  $\mathbf{p} \in \mathbb{S}$ , that the restriction of  $I$  to  $N_{20}(\mathbf{p})$  belongs to  $P$ . This LUT-based approach is formalised in Algorithm 3.

### 6.3 Parametrisation of the approach

The proposed approach for evaluating the topological invariance of digital images  $I$  defined on  $\mathbb{S}$ , under all DRTs, has been presented – for the sake of readability – in the classical framework of digital topology [24], *i.e.*, by considering binary images ( $|\mathbb{V}| = 2$ ), equipped with a standard pair of dual (8, 4)- or (4, 8)-adjacencies. Nevertheless, the nature (and thus the cardinality) of  $\mathbb{V}$ , such as the topological space used to equip  $\mathbb{S}$  with respect to  $\mathbb{V}$ , can be conveniently modified without loss of generality, making the proposed approach parametric from both the structural and the spectral points of view.

Indeed, on the one hand, the proposed algorithms (and in particular Algorithms 2 and 3) rely on the notion of DRT graph, that defines explicitly the structure of the transformed spaces, but neither the transformed images nor their associated value space  $\mathbb{V}$ , which are implicitly handled.

On the other hand, the topological space that is mapped on  $\mathbb{S}$  (and more generally on  $\mathbb{Z}^2$ ) with respect to  $\mathbb{V}$ , is only considered via the notion of simple point. More precisely, the only constraint related to the choice of the topology is the

necessity to characterise locally the preservation of homotopy-type, with respect to the images of  $\mathbb{S} \rightarrow \mathbb{V}$ .

Consequently, the proposed approach can be parametrized by a couple composed of (i) a value space  $\mathbb{V}$ , and (ii) a notion of simple point for the space of the images of  $\mathbb{S} \rightarrow \mathbb{V}$ .

Based on this assertion, several topological frameworks that provide different notions of simple point can be considered, including the following:

- binary images, equipped with the digital topology [24], deriving from the dual (4, 8)- or (8, 4)-adjacencies (proposed in this article);
- binary images, defined as well-composed sets [46], deriving from the (4, 4)-adjacencies;
- label images, defined as well-composed sets [35, 36], deriving from the (4, 4)-adjacencies;
- label images, equipped with the notion of digitally simple Xels [26] defined from the topology of cubical complexes;
- label images, equipped with the notion of simple point in covering images [47];
- grey-level images, equipped with the notion of  $\lambda$ -destructible point [34].

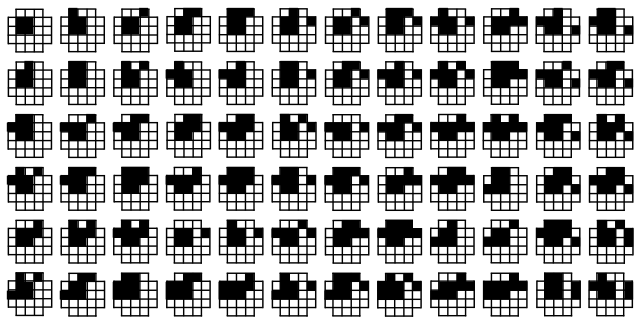
## 7 Analysis and experiments

In this section, we first analyse the complexity of the proposed algorithms. We then provide experiments devoted to validate the behaviour of the developed approach.

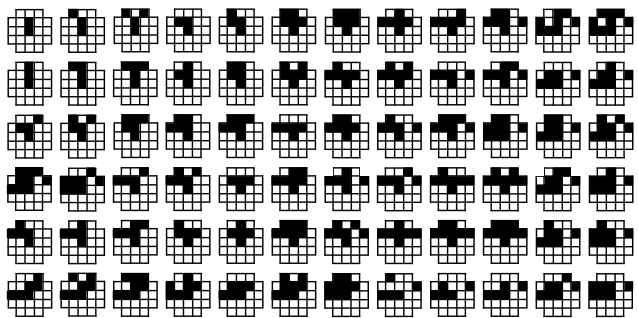
### 7.1 Theoretical complexity analysis

Given a digital image  $I$  of size  $N \times N$ , the first algorithm (Algorithm 1, in Sec. 5.2) relies on the DRT graph of  $I$ , and scans it entirely in the worst case. Consequently, both space and time complexities of this algorithm are  $O(N^9)$ , due to the space complexity of the DRT graph (Property 10).

The second algorithm (Algorithm 3, in Sec. 6.2) relies on (i) a LUT  $P$  of topology-preserving 20-neighbourhood images; and (ii) the verification of the compliance of  $I$  with  $P$  for any point of  $I$ . The generation of  $P$  (Algorithm 2, in Sec. 6.2), for a given value space  $\mathbb{V}$  and a given adjacency, has a time complexity  $O(5^9 |\mathbb{V}|^{20}) = O(|\mathbb{V}|^{20})$ , since the complexity for generating the DRT graph for an image defined on a 20-neighbourhood is  $O(5^9)$  [7], and any image  $I : N_{20}(\mathbf{0}) \rightarrow \mathbb{V}$  has to be processed via its DRT graph. Note however that this process has to be carried out only once, if  $P$  – that has a space complexity of  $O(|\mathbb{V}|^{20})$  – is stored. The topological invariance verification (Algorithm 3) then presents a quasi-linear time complexity with respect to the size  $N \times N$  of image  $O(N^2 \log_2(|P|)) = O(N^2 |\mathbb{V}|)$ , since the LUT  $P$  can be ordered and processed as a tree structure. One



(a)  $P$  in (4, 8)-adjacency (samples).



(b)  $P$  in (8, 4)-adjacency (samples).

**Fig. 11** Some samples defined on 20-neighbourhoods which are topology preserving, computed from Algorithm 2, in the case of (4, 8)-adjacency (a), and (8, 4)-adjacency (b). The foreground pixels are depicted in black, while the background pixels ( $\perp$ ) are depicted in white.

may notice that this algorithm can trivially be parallelized, leading in particular to a constant time complexity  $O(|\mathbb{V}|)$ , when processed as  $N^2$  subtasks.

### 7.2 Computational and space cost: The binary case

In this section, we experimentally assess the actual cost of the algorithm, previously discussed from a theoretical point of view. To this end, we consider the case of binary images, *i.e.*, images defined on a set of values  $\mathbb{V}$  such that  $|\mathbb{V}| = 2$ .

Let  $C$  be the set of all the binary images defined on  $N_{20}(\mathbf{0})$ , that is used to build  $P$  via Algorithm 2. We have, in particular,  $|C| = 2^{20}$ . However, from Remark 11, we only have to consider the images such that at least one point in the 4-neighbourhood of  $\mathbf{0}$  has a distinct (binary) value from the one of  $\mathbf{0}$ . By using this fact, plus considerations related to invariance up to rotations and symmetries, the set  $C$  can be reduced, without loss of completeness to a subset  $C' \subset C$  such that  $|C'| = 124\,260 \ll |C|$ .

Using Algorithm 2 on this set  $C'$ , we obtain some sets  $P$  of 10 643 and 19 446 elements, in the (4, 8)- and (8, 4)-adjacency, respectively. Fig. 11 provides some samples of  $P$  in both cases.

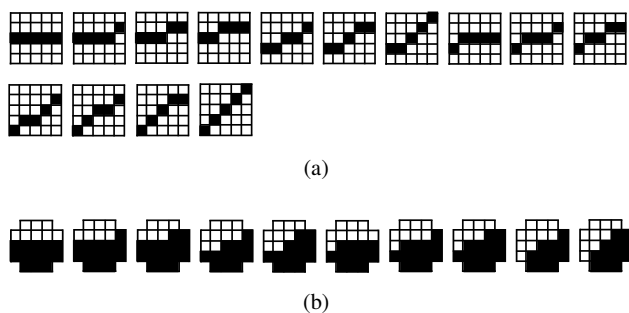


**Fig. 12** (a) The 14 samples of digital lines of length 5, and (b) the half-planes generated by these lines in a 20-neighbourhood.

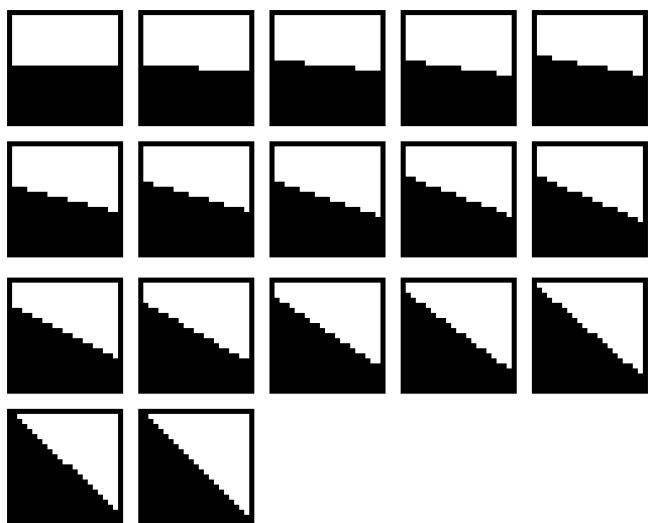


**Fig. 13** Some examples of half-planes rigidly transformed from an image of size  $20 \times 20$ . All transformed half-planes images are simple-equivalent.

### 7.3 Experiments: The binary case

We now propose some experiments to illustrate the behaviour of the algorithms on images representing different kinds of objects using the (4, 8)-adjacent relations. We first consider basic geometric primitives, namely half-planes and disks, the evolution of which is (in theory) predictable with respect to rigid transformations. Then, we consider more generally, arbitrary shapes, whose topological invariance is not easily predictable.

#### 7.3.1 Topological (in)variance of geometric primitives

We define a discrete half-plane as the set of all discrete points on one side of a digital straight line. The number of digital line segments was studied in [48]. In particular, it is known that there exist 14 digital segments of length 5 inside a pattern of size  $5 \times 5$  (see Fig. 12(a)). From this knowledge, we can generate all the possible half-planes in a 20-neighbourhood, as illustrated in Fig. 12(b). By using Algo-

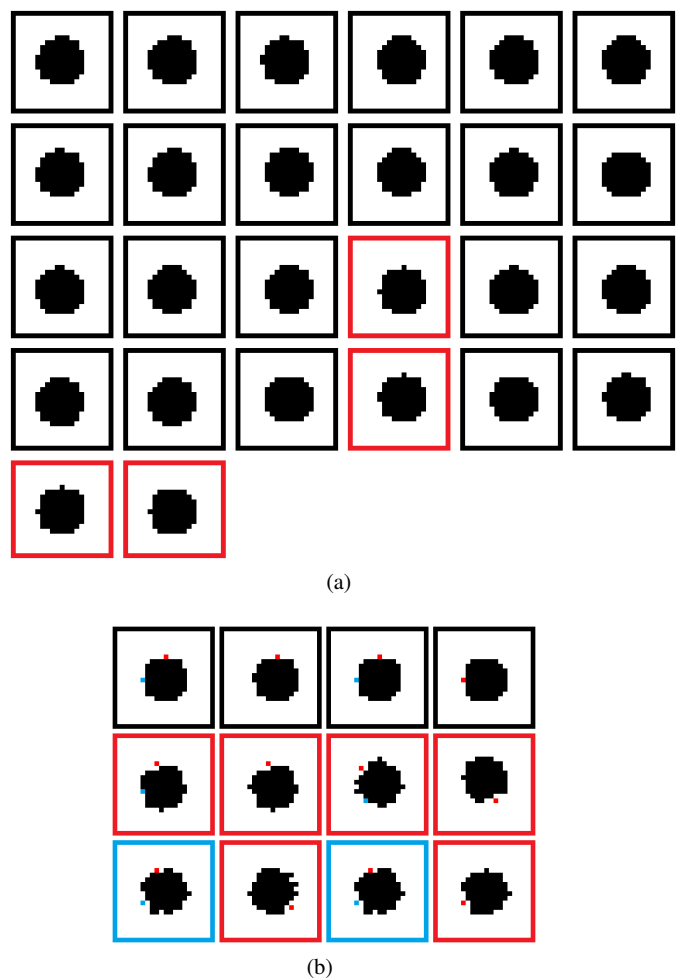


**Fig. 14** (a) Some disks of radius 5, generated in a image of size  $20 \times 20$ . Some of them are topologically invariant (in black frames), while the others (in red frame) have been characterised as not topologically invariant by Algorithm 3. (b) Concerning the four non topologically invariant disks in (a), the pixels detected by our algorithm are those that alter the topology of the four disks. The frame of the picture that surrounds them is coloured in red or blue according to the colour of the pixel for which the topology changes.

gorithm 2 to study the properties of these patterns, we find that all of them are topologically invariant. Therefore, we can conclude that any discrete half-plane preserves homotopy-type during digital/discrete rigid transformations. Some examples of rigidly transformed half-planes are illustrated in Fig. 13.

The digital disks, defined on  $\mathbb{Z}^2$  and studied, *e.g.*, in [49], can be defined as the sets of all discrete points lying inside a real disc (defined on  $\mathbb{R}^2$ ). It is plain that the digitization of a disc depends on its size (*i.e.*, its radius) but also on its position (*i.e.*, the position of its centre) with respect to the discrete grid. Some examples of digital disks with the same radius are shown in Fig. 14. In the continuous domain, the real disks are – of course – topologically invariant under rigid transformations. In contrast to the half-planes, this



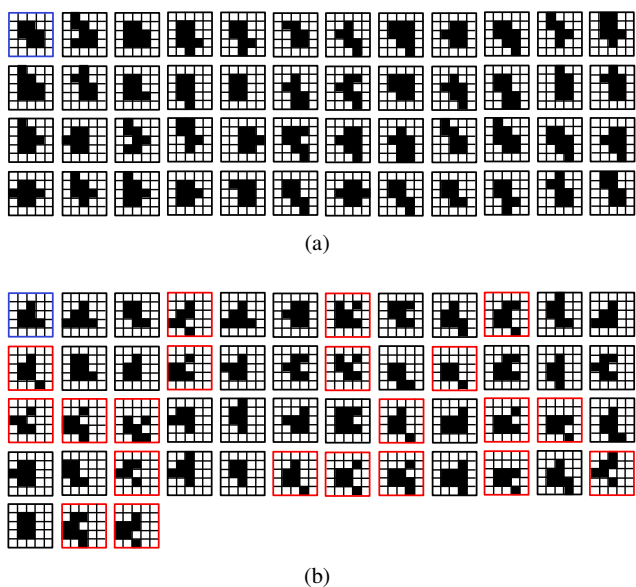


**Fig. 15** (a) A topologically invariant  $5 \times 5$  image (in blue frame), and (some of) its transformations (in black frames). (b) A topologically-variant  $5 \times 5$  image (in blue frame), and (some of) its simple-equivalent (in black frames) and non-simple-equivalent transformations (in red frames).

property is lost in the digital case. Indeed, Algorithm 3, performed on the images of Fig. 14, detects that some of them are not topologically invariant. This emphasizes the influence of the position of the disk center for this property. It also sheds light on the influence of the differential properties of the object boundaries – and in particular their curvature – on the potential preservation of image topology. From a methodological point of view, it can motivate the use of image simplification procedures that decompose boundaries into discrete line segments, since such approach may present more desirable topological properties.

### 7.3.2 Topological (in)variance of arbitrary shapes

To complete these experiments, we finally exhibit some examples of arbitrary binary images that have been characterised by Algorithm 3 as being topologically invariant (Figs. 15(a) and 16), or not (Figs. 15(b) and 17).

## 8 Conclusion

In this article, we have considered geometrical and topological concepts, to propose an approach for studying the topological behaviour of rigid transformations in  $\mathbb{Z}^2$ . More precisely, we combined the notion of simple point with the notion of DRT graph, leading to algorithmic processes that can characterise the topological invariance of digital images under *all* rigid transformations. In particular, by taking advantage of the respective strengths of both notions, it has

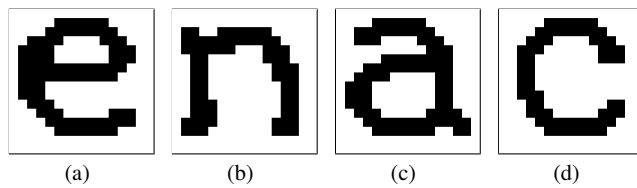


**Fig. 16** (a–d) Examples of topologically invariant character images.

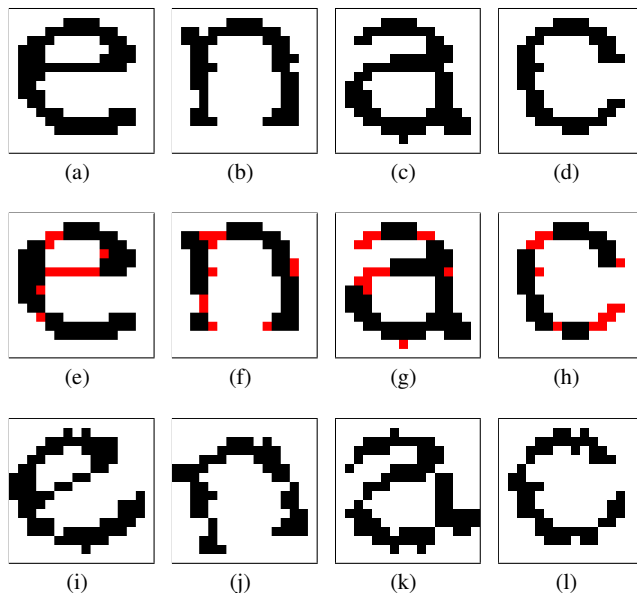


**Fig. 17** (a–d) Examples of non topologically invariant character images. (e–h) Detection of pixels (in red) which potentially change homotopy-type of (a–d) during DRTs. (i–l) Non-simple-equivalent transformed images of (a–d).

been possible to develop an efficient algorithm, able to evaluate this topological invariance in a quasi-linear time with respect to the image size.

Beyond its algorithmic aspects, this work may contribute to the better understanding of the relationships between geometry and topology in the framework of digital imaging, where both notions are less strongly linked than in the continuous space. In particular, the proposed algorithm may provide an efficient tool for further studying the notion of regularity [50–52], that is currently used to assess the preservation of topological properties during the digitization of an image from  $\mathbb{R}^2$  to  $\mathbb{Z}^2$ . In particular, a *discrete* notion of regularity may be derived from the continuous one, in order to assess the topological behaviour of image transformations in a fully discrete framework.

In this article, we have considered the specific case of the Eulerian transformation model (see Sec. 3.2). Further work may consider the case of the Lagrangian transformation model. In the context of topological alterations induced by rigid transformations of digital images, this latter model comes with some additional difficulties. Indeed, while in the Eulerian model, a double (resp. null) point transfers its



value to two (resp. no) point(s) in the transformed image (Sec. 4.2), in the Lagrangian case, a double (resp. null) point in the transformed image will receive two (resp. no) values; this leads to a result that is both incomplete and ambiguous. In order to deal with these supplementary issues, it may be necessary to study more deeply the relations that exist between the digital images, defined on  $\mathbb{Z}^2$ , and the continuous ones, defined on  $\mathbb{R}^2$ , as they are linked via the digitization processes.

## Acknowledgements

The research leading to these results has received partial funding from the French *Agence Nationale de la Recherche* (Grant Agreement ANR-10-BLAN-0205 03).

## References

1. B. Zitová, J. Flusser, Image registration methods: A survey, *Image and Vision Computing* 21 (11) (2003) 977–1000.
2. A. Yilmaz, O. Javed, M. Shah, Object tracking: A survey, *ACM Computing Surveys* 38 (4) (2006) 1–45.
3. V. Jain, B. Bollmann, M. Richardson, D. Berger, M. Helmstaedter, K. Briggman, W. Denk, J. Bowden, J. Mendenhall, W. Abraham, K. Harris, N. Kasthuri, K. Hayworth, R. Schalek, J. Tapia, J. Lichtman, S. Seung, Boundary learning by optimization with topological constraints, in: *CVPR, Proceedings, IEEE, 2010*, pp. 2488–2495.
4. S. Faisan, N. Passat, N. Noblet, R. Chabrier, C. Meyer, Topology preserving warping of 3-D binary images according to continuous one-to-one mappings, *IEEE Transactions on Image Processing* 20 (8) (2011) 2135–2145.
5. B. Dawant, S. Hartmann, J. Thirion, F. Maes, D. Vandermeulen, P. Demaerel, Automatic 3-D segmentation of internal structures of the head in MR images using a combination of similarity and free-form deformations: Part I, methodology and validation on normal subjects, *IEEE Transactions on Medical Imaging* 18 (10) (1999) 902–916.
6. P. Ngo, Y. Kenmochi, N. Passat, H. Talbot, Sufficient conditions for topological invariance of 2D digital images under rigid transformations, in: *DGCI, Proceedings, Vol. 7749 of Lecture Notes in Computer Science, Springer, 2013*, pp. 155–168.
7. P. Ngo, Y. Kenmochi, N. Passat, H. Talbot, Combinatorial structure of rigid transformations in 2D digital images, *Computer Vision and Image Understanding* 117 (4) (2013) 393–408.
8. M.-A. Jacob, E. Andres, On discrete rotations, in: *DGCI, Proceedings, 1995*, pp. 161–174.
9. A. Amir, O. Kapah, D. Tsur, Faster two-dimensional pattern matching with rotations, *Theoretical Computer Science* 368 (3) (2006) 196–204.
10. A. Amir, G. M. Landau, U. Vishkin, Efficient pattern matching with scaling, *Journal of Algorithms* 13 (1) (1992) 2–32.
11. A. Amir, A. Butman, M. Lewenstein, E. Porat, Real two dimensional scaled matching, *Algorithmica* 53 (3) (2009) 314–336.
12. C. Hundt, M. Liśkiewicz, N. Ragnar, A combinatorial geometrical approach to two-dimensional robust pattern matching with scaling and rotation, *Theoretical Computer Science* 410 (51) (2009) 5317–5333.
13. C. Hundt, M. Liśkiewicz, On the complexity of affine image matching, in: *STACS, Proceedings, Vol. 4393 of Lecture Notes in Computer Science, Springer, 2007*, pp. 284–295.
14. C. Hundt, Affine image matching is uniform  $TC^0$ -complete, in: *CPM, Proceedings, Vol. 6129 of Lecture Notes in Computer Science, Springer, 2010*, pp. 13–25.
15. C. Hundt, M. Liśkiewicz, Combinatorial bounds and algorithmic aspects of image matching under projective transformations, in: *MFCs, Proceedings, Vol. 5162 of Lecture Notes in Computer Science, Springer, 2008*, pp. 395–406.
16. J.-P. Reveillès, *Géométrie discrète, calcul en nombres entiers et algorithmique*, Thèse d'État, Université Strasbourg 1 (1991).
17. E. Andres, The quasi-shear rotation, in: *DGCI, Proceedings, Vol. 1176 of Lecture Notes in Computer Science, Springer, 1996*, pp. 307–314.
18. M. S. Richman, Understanding discrete rotations, in: *ICASSP, Proceedings, Vol. 3, IEEE, 1997*, pp. 2057–2060.
19. B. Nouvel, *Rotations discrètes et automates cellulaires*, Ph.D. thesis, École Normale Supérieure de Lyon (2006).
20. B. Nouvel, E. Rémila, Incremental and transitive discrete rotations, in: *IWCIA, Proceedings, Vol. 4040 of Lecture Notes in Computer Science, Springer, 2006*, pp. 199–213.
21. Y. Thibault, Y. Kenmochi, A. Sugimoto, Computing upper and lower bounds of rotation angles from digital images, *Pattern Recognition* 42 (8) (2009) 1708–1717.
22. G. Bertrand, On critical kernels, *Comptes Rendus de l'Académie des Sciences—Série Mathématiques I* (345) (2007) 363–367.
23. A. Rosenfeld, Connectivity in digital pictures, *Journal of the ACM* 17 (1) (1970) 146–160.
24. T. Y. Kong, A. Rosenfeld, Digital topology: Introduction and survey, *Computer Vision Graphics & Image Processing* 48 (3) (1989) 357–393.
25. L. Mazo, N. Passat, M. Couprie, C. Ronse, Paths, homotopy and reduction in digital images, *Acta Applicandae Mathematicae* 113 (2) (2011) 167–193.
26. L. Mazo, N. Passat, M. Couprie, C. Ronse, Digital imaging: A unified topological framework, *Journal of Mathematical Imaging and Vision* 44 (1) (2012) 19–37.
27. E. Khalimsky, Topological structures in computer science, *Journal of Applied Mathematics and Simulation* 1 (1) (1987) 25–40.
28. V. A. Kovalevsky, Finite topology as applied to image analysis, *Computer Vision, Graphics & Image Processing* 46 (2) (1989) 141–161.
29. G. Bertrand, G. Malandain, A new characterization of three-dimensional simple points, *Pattern Recognition Letters* 15 (2) (1994) 169–175.
30. M. Couprie, G. Bertrand, New characterizations of simple points in 2D, 3D, and 4D discrete spaces, *IEEE Transactions on Pattern Analysis and Machine Intelligence* 31 (4) (2009) 637–648.
31. C. Ronse, A topological characterization of thinning, *Theoretical Computer Science* 43 (1) (2007) 31–41.
32. G. Bertrand, On P-simple points, *Comptes Rendus de l'Académie des Sciences—Série Mathématiques I* (321) (1995) 1077–1084.
33. N. Passat, L. Mazo, An introduction to simple sets, *Pattern Recognition Letters* 30 (15) (2009) 1366–1377.
34. M. Couprie, F. N. Bezerra, G. Bertrand, Topological operators for grayscale image processing, *Journal of Electronic Imaging* 10 (4) (2001) 1003–1015.
35. L. J. Latecki, Multicolor well-composed pictures, *Pattern Recognition Letters* 16 (4) (1997) 425–431.
36. G. Damiand, A. Dupas, J.-O. Lachaud, Fully deformable 3D digital partition model with topological control, *Pattern Recognition Letters* 32 (9) (2011) 1374–1383.
37. L. Mazo, N. Passat, M. Couprie, C. Ronse, Topology on digital label images, *Journal of Mathematical Imaging and Vision* 44 (3) (2012) 254–281.
38. D. Pham, P.-L. Bazin, J. Prince, Digital topology in brain imaging, *IEEE Signal Processing Magazine* 27 (4) (2010) 51–59.

- 
39. J.-F. Mangin, V. Frouin, I. Bloch, J. Régis, J. López-Krahe, From 3D magnetic resonance images to structural representations of the cortex topography using topology preserving deformations, *Journal of Mathematical Imaging and Vision* 5 (4) (1995) 297–318.
  40. X. Han, C. Xu, J. L. Prince, A topology preserving level set method for geometric deformable models, *IEEE Transactions on Pattern Analysis and Machine Intelligence* 25 (6) (2003) 755–768.
  41. P.-L. Bazin, L. M. Ellingsen, D. L. Pham, Digital homeomorphisms in deformable registration, in: *IPMI, Proceedings*, Vol. 4584 of *Lecture Notes in Computer Science*, Springer, 2007, pp. 211–222.
  42. R. Ayala, E. Domínguez, A. R. Francés, A. Quintero, Homotopy in digital spaces, *Discrete Applied Mathematics* 125 (1) (2003) 3–24.
  43. G. Bertrand, M. Couprie, N. Passat, A note on 3-D simple points and simple-equivalence, *Information Processing Letters* 109 (13) (2009) 700–704.
  44. B. Nouvel, E. Rémila, Configurations induced by discrete rotations: Periodicity and quasi-periodicity properties, *Discrete Applied Mathematics* 147 (2–3) (2005) 325–343.
  45. Y. Thibault, Rotations in 2D and 3D discrete spaces, Ph.D. thesis, Université Paris-Est (2010).
  46. L. J. Latecki, U. Eckhardt, A. Rosenfeld, Well-composed sets, *Computer Vision and Image Understanding* 61 (1) (1995) 70–83.
  47. L. Mazo, A framework for label images, in: *CTIC, Proceedings*, Vol. 7309 of *Lecture Notes in Computer Science*, Springer, 2012, pp. 1–10.
  48. C. Berenstein, D. Lavine, On the number of digital straight line segments, *IEEE Transactions on Pattern Analysis and Machine Intelligence* 10 (6) (1988) 880–887.
  49. B. Nagy, An algorithm to find the number of the digitizations of discs with a fixed radius, *Electronic Notes in Discrete Mathematics* 20 (2005) 607–622.
  50. J. Serra, *Image Analysis and Mathematical Morphology*, Academic Press, Inc., 1983.
  51. H. J. A. M. Heijmans, Discretization of morphological operators, *Journal of Visual Communication and Image Representation* 3 (2) (1992) 182–193.
  52. L. J. Latecki, C. Conrad, A. Gross, Preserving topology by a digitization process, *Journal of Mathematical Imaging and Vision* 8 (2) (1998) 131–159.